The magnetophonon modes of a three-dimensional Wigner crystal in a magnetic field

1992 J. Phys.: Condens. Matter 4 1251

(http://iopscience.iop.org/0953-8984/4/5/005)

J. Phys.: Condens. Matter 4 (1992) 1251–1262. Printed in the UK

The magnetophonon modes of a three-dimensional Wigner crystal in a magnetic field

D A Browne

Department of Physics and Astronomy, Louisiana State University, Baton Rouge, LA 70803-4001, USA

Received 22 April 1991, in final form 1 October 1991

Abstract. We calculate the transverse phonon spectrum of a three-dimensional Wigner crystal in a large magnetic field where the electrons occupy the lowest spin-polarized Landau level. The calculation differs from that for a conventional phonon spectrum because the lattice is stable only in the presence of the magnetic field. We give specific results for wavevectors parallel and perpendicular to the magnetic field for the phonon spectrum of a Wigner crystal state in the narrow gap semiconductor HgCdTe. The temperature dependence of the electron lattice specific heat is also calculated and varies as $T^{3/2}$.

1. Introduction

Since the original prediction by Wigner [1] that a low density electron gas at zero temperature should crystallize into a solid, much theoretical effort [2–6] has been devoted to understanding its properties. The crystalline state occurs when the electrostatic repulsion dominates the kinetic energy and the electrons localize to minimize the Coulomb interaction. In the very low density and finite temperature regime, the kinetic energy is entirely due to thermal motion and the formation of the crystal is similar to classical crystallization. At higher densities, it is the zero point motion of the electrons that competes with the Coulomb repulsion. If the density is high enough, the zero point energy is large enough to suppress the crystallization and a metallic state with delocalized electrons results at zero temperature.

Although there is currently no direct evidence for the three-dimensional quantum crystal, there have been numerous studies of the two-dimensional crystal, where the electrons form a triangular lattice [7]. Grimes and Adams [8] succeeded in producing a classical two-dimensional crystal in a monolayer of electrons confined to the surface of liquid helium. However, it is not possible to raise the electron density in this system sufficiently to study the quantum crystal because the electrons induce an instability in the helium surface. Dahm and co-workers [9] have studied electrons over a thin layer of helium on substrates like glass and have reached densities comparable to the crystallization point, but the surface is more disordered than the liquid He surface and high mobilities are hard to achieve. Another system that has been studied in some detail is the two-dimensional electron gas in a semiconductor heterojunction, but it has not been possible to reduce the electron density sufficiently to study the quantum melting because the scattering from the dopant impurities and surface defects proved strong enough to localize the carriers.

0953-8984/92/051251+12$04.50

It was suggested by Durkan *et al* [10] that the crystal would form more easily in a magnetic field. By applying a magnetic field of sufficient strength to put all the electrons in the lowest Landau level, the kinetic energy of motion perpendicular to the field would be quenched, and the critical electron density for crystallization would increase to a more accessible value. For a two-dimensional system where the motion along the field is also quantized, this Wigner crystal state will compete with the quantum liquid state of the fractional quantum Hall effect [11]. Except in the immediate vicinity of Landau filling fractions with a small odd denominator, current theoretical estimates [12] give a crystalline ground state for all filling factors of less than about 0.15, which is in accord with several recent measurements [13] on semiconductor heterojunctions.

The three-dimensional electron gas in a magnetic field has also been studied extensively. Kaplan and Glasser [14] suggested that the electrons crystallize into one-dimensional rods of electron gases oriented along the magnetic field. Kleppman and Elliot [15] found that the ground state energy could be improved by localizing the charge along the rods in the form of a charge density wave (CDW). It was assumed [16, 17] that the evolution from a CDW state to a Wigner crystal with well localized charge is continuous. However, MacDonald and Bryant [18], improving on previous work by including exchange interactions, found a wide variety of crystalline phases for varying magnetic field that differed in the degree of localization of the charge along the field. They found rod-like states, CDW states with a small modulation of the charge density along the field and a crystalline state with the electron charge well localized inside the unit cell.

There have been several experimental studies of three-dimensional Wigner crystallization in a high field. Early studies of n-InSb [19] were claimed to show some evidence for a magnetic-field-induced Wigner crystal [6, 10, 15] and it has been postulated [20] that a Wigner crystal could form in the core of a white dwarf. Rosenbaum and co-workers [21] and Schlicht and Nimtz [22] performed a series of magnetotransport measurements that they claimed were evidence for a three-dimensional Wigner transition in the narrow gap semiconductor HgCdTe in a high magnetic field. However, there remains considerable controversy over whether the transition in HgCdTe, which has also been seen in heat capacity [23] and spin resonance [24] experiments, is better described as a magnetic-field-induced Mott transition [25] or magnetic freeze-out [26].

What is needed is clear experimental evidence of the crystalline nature if this controversy is to be resolved. Since the electron spacing in the crystal is typically 800 Å, neutron scattering [27] or ultraviolet light scattering could in principle be used. However, the fundamental property of the solid state is a finite resistance to shear, so a clear sign of the formation of a solid would be the detection of the transverse collective modes of the solid. While both a glassy state induced by disorder [28] and the Wigner state could be expected to show a finite shear modulus, a crystal is unique in that the phonon modes can show considerable *anisotropy* due to the reduced symmetry.

Therefore, an unambiguous signal of the crystalline state would be the detection of anisotropy in the transverse modes. Since the electrons are moving against a rigid background, the modes could be detected by coupling to them with an electric field of the correct frequency. This could be done either with a meander line or by using ultrasound if the underlying medium is a piezoelectric semiconductor.

In this paper we will examine the transverse modes of a three-dimensional Wigner

crystal in a high magnetic field, with particular attention being paid to the anisotropy in the modes. We shall see that, since the magnetic field produces much of the stability of the lattice, the phonon modes differ in several respects from the usual phonon modes [15, 29, 30] in the absence of the field. We will use material parameters appropriate for HgCdTe to compute an actual phonon spectrum, although the technique can be applied to a variety of materials. We will restrict ourselves to the simplest crystal structures, a centred tetragonal structure and a hexagonal-close-packed (HCP) structure where the electron charge is well localized in all three directions. We expect that the results found here are also qualitatively correct in the other states found by Kaplan and Glasser [14] and MacDonald and Bryant [18] where the electron charge is more extended along the field.

This paper is divided into four parts. In section 2 we set forth our technique for calculating the phonon spectrum. Section 3 will present the results for HgCdTe with the Wigner crystal in a centred tetragonal structure, since variational calculations [15] seem to label this as the preferred ground state at zero temperature. We will discuss the differences expected for the glassy state and for the other hypothesized [6, 15] crystalline form, the HCP crystal. Section 4 contains the conclusions.

2. Formalism

We consider a system of electrons localized near sites R_i which form a regular three-dimensional lattice. The electrons experience a uniform magnetic field in the z-direction, which is described by a vector potential $A = (B/2)(-y, x, 0)$. The electrons interact with each other through a mutual Coulomb repulsion and with a rigid background charge of magnitude e/Ω, where Ω is the volume of a unit cell of the lattice. The Hamiltonian of the system is

$$\begin{aligned}\mathcal{H} = {} & \frac{1}{2m^*}\sum_i \left(p_i - \frac{e}{c}A(R_i + u_i)\right)^2 \\ & - \frac{e^2}{\epsilon_0}\sum_i \int \frac{\mathrm{d}\rho}{\Omega}\left(\frac{1}{|u_i - \rho|} - \frac{1}{2}\int \frac{\mathrm{d}\rho'}{\Omega}\frac{1}{|\rho - \rho'|}\right) \\ & + \frac{e^2}{2\epsilon_0}\sum_{i\neq k}\frac{1}{|R_{ik} - u_i + u_k|} \\ & - \frac{e^2}{2\epsilon_0}\sum_{i\neq k}\int \frac{\mathrm{d}\rho}{\Omega}\left(\frac{1}{|R_{ik} - u_i + \rho|} + \frac{1}{|R_{ik} - \rho + u_k|}\right) \\ & + \frac{e^2}{2\epsilon_0}\sum_{i\neq k}\int \frac{\mathrm{d}\rho}{\Omega}\int \frac{\mathrm{d}\rho'}{\Omega}\frac{1}{|R_{ik} - \rho + \rho'|} \end{aligned} \tag{1}$$

where m^* is the effective mass of the electron, ϵ_0 is the background dielectric constant, u_i is the coordinate of the ith electron relative to the centre of the cell R_i, $R_{ik} = R_i - R_k$ is the distance between the centres of the two cells, and $\int \mathrm{d}\rho/\Omega$ denotes an integration over the uniform background charge in a single unit cell. Because each cell is electrically neutral, the largest interaction is between the electron in a given cell and the uniform background charge in that cell [5, 17], which is given

by the second term in (1). The interaction between the electrons and associated background charge in different cells, contained in the last three terms of (1), is much smaller, the two leading terms being a dipole–dipole (van der Waals) term and a quadrupole electrostatic term.

In order to calculate the restoring force due to the Coulomb interaction, we need a good description of the electronic charge distribution in the cell. We will get this by a technique used by Kuramoto [17] for calculating the ground state energy of the crystal. Since the intercell interaction is small [5, 17], we will ignore it and consider only the interaction with the background charge in the Wigner–Seitz cell. We replace the cell by a prolate ellipsoid with the same volume. The potential of such a uniformly charged ellipsoid, including the Madelung energy of the background, is given by

$$V(r) = -\frac{e^2}{\epsilon_0}\int \frac{d\rho}{\Omega}\frac{1}{|r-\rho|} + \frac{e^2}{2\epsilon_0}\int\frac{d\rho}{\Omega}\int\frac{d\rho'}{\Omega}\frac{1}{|\rho-\rho'|} \tag{2}$$

where the integration is over the region $(x^2+y^2)/a^2 + z^2/c^2 < 1$, and c and a are the major and minor axes of the ellipsoid. The integral can be done in closed form to yield

$$V(r) = \frac{1}{2}m^*\omega_p^2\left\{\frac{x^2+y^2}{2\gamma(\gamma^2-1)}\left(\gamma - \frac{\cosh^{-1}(\gamma)}{\sqrt{\gamma^2-1}}\right) + \frac{z^2\gamma}{\gamma^2-1}\left(\frac{\cosh^{-1}(\gamma)}{\sqrt{\gamma^2-1}} - \frac{1}{\gamma}\right) - \frac{3}{5}a^2\gamma\frac{\cosh^{-1}(\gamma)}{\sqrt{\gamma^2-1}}\right\} \tag{3}$$

where $\gamma = c/a$ and $\omega_p^2 = 4\pi ne^2/\epsilon_0 m^*$ is the square of the plasma frequency with an electron density of $n = 1/\Omega$. Since we will find that the electron is localized well inside the cell, we can ignore the boundary. The resulting Schrödinger equation with this potential and the kinetic energy term from (1) is simply an anisotropic harmonic oscillator in a magnetic field. If we define raising and lowering operators by $x \pm iy = \sqrt{(\hbar/m^*\Omega_\perp)}(A_\pm + A_\pm^\dagger)$ and $z = \sqrt{(\hbar/2m^*\omega_z)}(A_z + A_z^\dagger)$, where $\Omega_\perp^2 = (\omega_c/2)^2 + \omega_\perp^2$ and $\omega_c = (eB/m^*c)$ is the cyclotron frequency, the Hamiltonian can be diagonalized to yield

$$H = -V_0 + \hbar\left(\Omega_\perp + \frac{\omega_z}{2}\right) + \hbar\left(\Omega_\perp + \frac{\omega_c}{2}\right)A_+^\dagger A_+ + \hbar\left(\Omega_\perp - \frac{\omega_c}{2}\right)A_-^\dagger A_- + \hbar\omega_z A_z^\dagger A_z \tag{4}$$

where V_0 is the constant term in (3). The ground state wavefunction for an electron at site R_i is given by

$$\psi_0(r) = \frac{1}{\sqrt{2\pi^{1/2}\alpha_\perp^2\alpha_z}}\exp\left(-\frac{x^2+y^2}{4\alpha_\perp^2} - \frac{z^2}{4\alpha_z^2} - i(R_i \times r)\cdot\hat{z}\right) \tag{5}$$

where $\alpha_\perp^2 = \hbar/(2m^*\Omega_\perp)$ and $\alpha_z^2 = \hbar/(2m^*\omega_z)$. We now adjust γ so as to minimize the ground state energy [17], including the zero point energy. This yields a variational estimate of the ground state charge distribution. Plots of the resulting values for c, a, $\alpha_\perp$ and α_z are given in figure 1. For large fields, $\alpha_\perp$ approaches the magnetic length

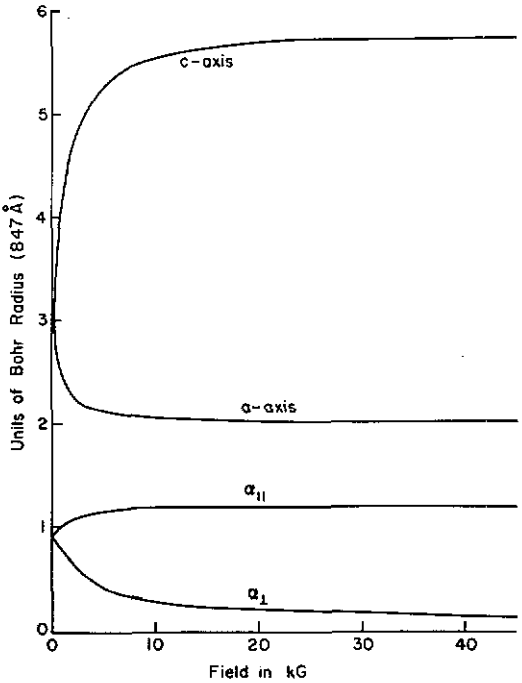

Figure 1. The variation of the unit cell dimensions (a, c) and the dimensions of the charge distribution in the unit cell with magnetic field. The results shown apply to the case of HgCdTe with a carrier density of 1.4×10^{14} cm^{-3} as studied in [21].

$\sqrt{(hc/eB)}$ [17]. We also see that the charge distribution is well localized inside the cell, and is an elongated ellipsoid oriented along the field in a unit cell with a ratio of sides that is similar to the ratio of the dimensions of the charge distribution.

In order to account for the long range correlations due to the interactions, that have so far been neglected in our single particle picture, we include the van der Waals interaction between the localized charges. We use the usual expression [31] for the van der Waals interaction given by

$$E_{\mathrm{VdW}} = \frac{e^4}{R^6} \sum_i \frac{|\langle 0|(\boldsymbol{r}\cdot\boldsymbol{r}') - 3(\boldsymbol{r}\cdot\hat{\boldsymbol{R}})(\boldsymbol{r}'\cdot\hat{\boldsymbol{R}})|i\rangle|^2}{E_0 - E_i} \tag{6}$$

where the set $|i\rangle$ denotes all excited states with energy E_i of the two electrons with coordinates $\boldsymbol{r}$, $\boldsymbol{r}'$ in cells a distance $\boldsymbol{R}$ apart and $\hat{\boldsymbol{R}}$ is a unit vector. We use the Hamiltonian of (4) to calculate the van der Waals interaction. If θ denotes the angle between $\boldsymbol{R}$ and the z-axis, we find the following form for the interaction in the limit $\omega_c \gg \omega_p$

$$E_{\mathrm{VdW}} = \frac{e^2}{R^6} \frac{\alpha_z^4}{2\omega_z} \left(1 - 3\cos^2\theta\right)^2 . \tag{7}$$

Since we now have a reasonable approximation to the electron wavefunction in a single cell, we will be able to calculate the restoring force on the phonon. We take as the ground state wavefunction a product of the single cell wavefunctions [15, 17], one for each cell. In what follows we will ignore the exchange interaction since it can be

shown [15] to be very small for the range of magnetic fields we will consider. We can also ignore the non-orthogonality of the wavefunctions in different cells since it is of the same order of magnitude as the exchange corrections [15]. We will use a 'rigid ion' approximation where the electron has the same wavefunction as in the ground state, except that it is displaced from the cell centre. The equation of motion for the electron displacement $d_\alpha(\boldsymbol{q},\omega)\exp(\mathrm{i}(\boldsymbol{q}\cdot\boldsymbol{R}_i-\omega t)$ can be written [29]

$$\omega^2 d_\alpha = \mathrm{i}\omega_c\omega\epsilon_{\alpha\beta 3}d_\beta + D_{\alpha\beta}(\boldsymbol{q})d_\beta - \frac{e}{m^*}(E_\alpha^{\mathrm{mac}}(\boldsymbol{q},\omega)+E_\alpha^{\mathrm{ext}}(\boldsymbol{q},\omega)) \tag{8}$$

where $\epsilon_{\alpha\beta\gamma}$ is the antisymmetric matrix and $D_{\alpha\beta}(\boldsymbol{q}) = D_{\alpha\beta}^{\mathrm{Coul}}(\boldsymbol{q}) + D_{\alpha\beta}^{\mathrm{VdW}}(\boldsymbol{q})$ is the dynamical matrix arising from the Coulomb repulsion and the van der Waals interaction. Because the background is rigid, the electronic motion is accompanied by a macroscopic electric field [29, 32], which we have removed from the Coulomb contribution to the dynamical matrix and written E^{mac}. E^{ext} is an externally applied field. If $\rho(\boldsymbol{q})$ denotes the Fourier transform of the charge distribution in a cell, and we define $F_{\alpha\beta}(\boldsymbol{q}) = |\rho(\boldsymbol{q})|^2 q_\alpha q_\beta/q^2$, the Coulomb contribution to the dynamical matrix is given by

$$D_{\alpha\beta}^{\mathrm{Coul}}(\boldsymbol{q}) = \omega_p^2\left[F_{\alpha\beta}(\boldsymbol{q}) - \frac{q_\alpha q_\beta}{q^2} + \sum_{\boldsymbol{\tau}\neq 0}\{F_{\alpha\beta}(\boldsymbol{\tau}+\boldsymbol{q}) + F_{\alpha\beta}(\boldsymbol{\tau}-\boldsymbol{q}) - 2F_{\alpha\beta}(\boldsymbol{\tau})\}\right] \tag{9}$$

where the sum is over all non-zero reciprocal lattice vectors $\boldsymbol{\tau}$.

From Maxwell's equations E^{mac} obeys the equation of motion [29, 32]

$$[(\omega^2 - u^2q^2)\delta_{\alpha\beta} + u^2 q_\alpha q_\beta]E_\beta^{\mathrm{mac}} = -4\pi\omega^2 P_\alpha \tag{10}$$

where $P_\alpha = ned_\alpha$ is the macroscopic polarization and $u = c/\sqrt{\epsilon_0}$ is the speed of light in the medium. We will consider only modes where $\omega \ll uq$. The van der Waals attraction gives a contribution to $D_{\alpha\beta}$ of the form

$$D_{\alpha\beta}^{\mathrm{VdW}}(\boldsymbol{q}) = \frac{1}{m^*}\sum_{\boldsymbol{R}\neq 0}\frac{\partial^2}{\partial R_\alpha \partial R_\beta}\{E^{\mathrm{VdW}}(\boldsymbol{R})[1-\exp(\mathrm{i}\boldsymbol{q}\cdot\boldsymbol{R})]\} \tag{11}$$

Combining (8) and (10) yields a phonon equation of motion of the form

$$\left[\omega^2\left(1+\left(\frac{\omega_p}{uq}\right)^2\right)\delta_{\alpha\beta} - \mathrm{i}\omega\omega_c\epsilon_{\alpha\beta 3} - D_{\alpha\beta} - w_p^2\frac{q_\alpha q_\beta}{q^2}\right]d_\beta(\boldsymbol{q},\omega) = -\frac{e}{m^*}E_\alpha^{\mathrm{ext}}(\boldsymbol{q},\omega). \tag{12}$$

The dispersion relationships for the collective modes can be found by finding the frequencies where the determinant of the right-hand side of (12) vanishes. There are two special cases, $\boldsymbol{q} = (0,0,q)$ and $\boldsymbol{q} = (q_x, q_y, 0)$, where the frequency of the

modes is easily found in closed form. For the case of q parallel to the z-axis we find, in addition to the usual helicon mode, an additional transverse mode circularly polarized in the x–y plane in the opposite sense to the helicon with the dispersion relationship

$$\omega = \frac{D_{11}(q)}{\omega_c}. \tag{13}$$

For the case of q in the x–y plane, there are two low-frequency transverse modes. There is one transverse mode polarized in the z-direction with dispersion relationship

$$\omega^2 = \frac{u^2q^2}{\omega_p^2 + u^2q^2} D_{33}(q) \tag{14}$$

and one with polarization $\hat{e} = \hat{z} \times q$.

$$\omega^2 = \frac{u^2q^2}{\omega_p^2 + u^2q^2} \frac{u^2\omega_p^2}{\omega_p^2 + u^2q^2(\omega_p^2 + \omega_c^2)} (q_y^2 D_{11}(q) + q_x^2 D_{22}(q) + 2q_x q_y D_{12}(q)). \tag{15}$$

These dispersion relationships were derived by Kuramoto [29] in a slightly different form. He assumed that the dynamical matrix could be written in terms of a set of conventional elastic constants. In the present situation, however, it is not possible to write elastic moduli for the Coulomb restoring force for two reasons. First, if one were to write the dynamical matrix **D**, which is of order q^2 as $q \to 0$, as a sum of various elastic terms, the elastic 'constants' would actually depend [32] on the direction of q if the symmetry of the lattice were less than cubic, as it is here. These effects occur because of the long range of the Coulomb interaction. Second, the Coulomb energy in (3) is minimized if $\gamma = 1$, that is if the lattice is isotropic. The large anisotropy induced by the magnetic field results in the dynamical matrix being evaluated in a charge configuration which is so far from its stable minimum (as far as the Coulomb repulsion is concerned) that several of the elastic constants are negative or fail to satisfy the conventional stability criteria [32]. We have therefore avoided introducing elastic constants in this discussion.

We also have not restricted our discussion to a particular lattice structure so far, although we have assumed that there is only one electron per unit cell. Indeed, our use of an ellipsoid for the Wigner–Seitz cell could approximate the unit cell of any lattice with higher than two-fold symmetry about the z-axis. On the basis of variational calculations [15] at zero temperature, either the centred tetragonal structure or the HCP lattice are possible ground states, with the former having a slightly lower energy. We will present detailed results only for the centred tetragonal structure, and will describe qualitatively the differences for the HCP structure.

We have not described here the longitudinal modes of the lattice, since the rigid background causes them to lie at the plasma frequency and act like an optic mode [2]. There are also higher electromagnetic modes that come from solving (8) and (10) without the approximation $\omega \ll uq$, but they are not significantly perturbed by the presence of the lattice. Since the electrons are localized, and the longitudinal modes occur at the plasma frequency, the only low-lying excitations of the Wigner crystal are the transverse phonons. Thus the specific heat of the crystal will be dominated

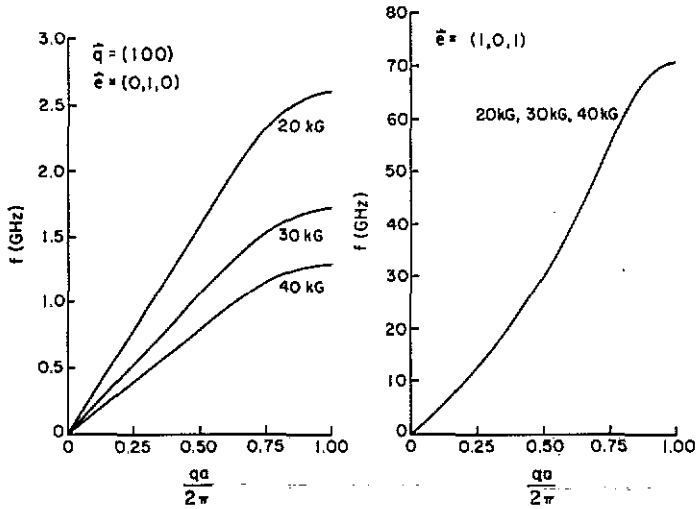

Figure 2. The phonon spectrum for transverse modes with q in the (100) direction for the centred tetragonal structure. Results for three values of magnetic field are presented (20, 30 and 40 kG). Note the peculiar upward curvature of the z-polarized mode.

by the contribution from these transverse modes. From (13), (14) and (15) we see that the dispersion of these modes at small q is quadratic, rather than linear, so the temperature dependence of the specific heat will be different from that of a Debye model.

If there is a low-lying mode with dispersion relationship $\omega = Gq^p$, as $q \to 0$, where G and p are constants, it will contribute to the low-temperature heat capacity a term of the form

$$C = \frac{Vk_B}{(2\pi)^3}\frac{3+p}{p^2}\Gamma\left(1+\frac{3}{p}\right)\zeta\left(1+\frac{3}{p}\right)\int dS\left(\frac{k_B T}{hG}\right)^{3/p} \tag{16}$$

where V is the volume, $\int dS$ denotes an integral over all solid angles, $\Gamma(x)$ is the gamma function, $\zeta(x)$ is the Riemann zeta function, and we have assumed the system is three-dimensional. Each independent mode will give a separate term of this form. It is obvious that the modes with the largest value of p and the smallest G will dominate the expression for the specific heat as $T \to 0$. As we will see later, the 'anti-helicon' mode with the dispersion relationship given by (13) will give the largest contribution because the magnetic field (and therefore ω_c) is large and $D_{11}(q) \sim q^2$ with a small coefficient. Therefore we expect the specific heat to vary as $T^{3/2}$ at low temperatures and also vary as $H^{3/2}$ with magnetic field. In a similar fashion, we expect the thermal conductivity to show the same kind of temperature and field dependence.

3. Results

For the HgCdTe samples used in the experiments performed by Rosenbaum *et al* [21], the effective mass was about 1/80 of an electron mass, the electron density was

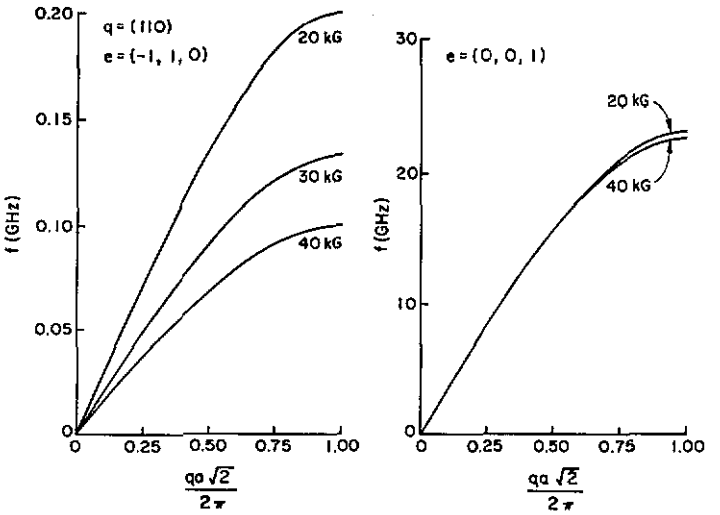

Figure 3. The phonon spectrum for transverse modes with q in the (110) direction for the centred tetragonal structure. Results for three values of magnetic field are presented (20, 30 and 40 kG). If the crystal structure were hexagonal there would be no difference between the (110) and (100) directions.

1.40×10^{14} cm^{-3}, and the dielectric constant was about 20. These values result in a plasma frequency of 210 GHz and a cyclotron frequency in a 10 kG field of 2200 Ghz.

In figure 2 we show results for the transverse phonon modes at three values of magnetic field for q along the (100)-axis and in figure 3 the modes for q along the (110)-axis. The modes along the (100) direction show a peculiar upward curvature about halfway to the edge of the zone, an effect which is also seen in the two-dimensional Wigner crystal [7, 33]. In figure 4 we show the phonons along the (001) direction. For the range of fields and q values shown here, we have ω_c, $uq \gg \omega_p$. The actual frequencies calculated here are about an order of magnitude smaller than those estimated by Kuramoto [29]. This is due to the fact that the restoring force for the transverse modes actually vanishes [32] for a set of point charges in a cubic lattice, so the magnitude of the restoring force is sensitive to the precise form of the charge distribution. For the modes shown here, even those that seem linear for small q actually have a region where ω varies as q^2, but it is too close to the origin to be visible. This quadratic behaviour results from the large magnetic field present.

It is easily seen that the four-fold symmetry about the z-axis in the centred tetragonal structure leaves considerable anisotropy as q varies in the x–y plane. From (16) it is simple to show that the variation of frequency of the mode where $\hat{e} = \hat{z} \times q$ with azimuthal angle ϕ is given by $\omega^2 = \omega_0^2 - \omega_1^2 \sin^2(2\phi)$ where from figures 2 and 3 we find ω_1 is approximately $0.7\omega_0$. If this anisotropy could be detected, it would be a clear signal of the presence of the Wigner crystal state. If the crystal structure is HCP, however, this anisotropy is not present and it would be impossible to show that the crystalline state was present instead of a glassy state that might result if the disorder predominated. The change in the frequency of the modes with field can be traced almost entirely to the presence or absence of a factor of ω_c in (13), (14) and

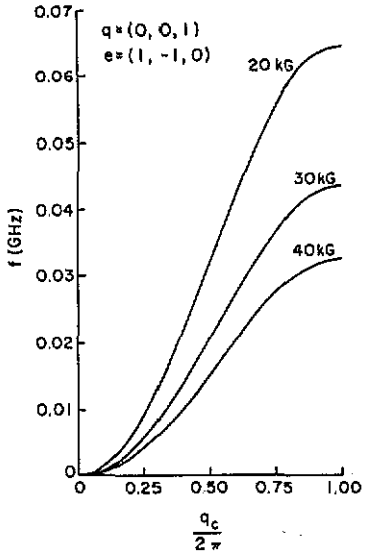

Figure 4. The phonon spectrum for transverse modes with q in the (001) direction for the centred tetragonal structure. Results for three values of magnetic field are presented (20, 30 and 40 kG).

(15). The values of $D_{\alpha\beta}$ are very slowly varying with the magnetic field, which can be explained from figure 1 by the slow variation of the charge distribution with field in the range we have presented here. This is clearly seen in the figure 3 for the mode polarized along the z-axis.

In figure 5 we present calculations of the variation of the frequency of a transverse mode with the angle relative to the magnetic field. For q along (001) the mode has a polarization opposite to the helicon mode, which means that the magnetic field softens the mode (which is the reason ω_c appears in the denominator of (13)). Since the magnetic energy is so large, the softening effect of the field disappears only when q is nearly perpendicular to the field. This explains the rapid rise in the frequency of the mode near the (100) direction. The rest of the variation of the mode with polar angle is simply due to the anisotropy of the lattice. The case of the hexagonal lattice will show similar behaviour to that presented here for the centred tetragonal lattice.

Figure 5 shows that the 'anti-helicon' mode dispersion relationship given in (13) holds well provided q is not exactly perpendicular to the field, so we can use (13) to calculate the specific heat at low temperature. We find that the lattice specific heat per electron is roughly $C/Nk_B = 8.6 \times 10^3(H(\mathrm{T})/T(\mathrm{K}))^{3/2}$ for the region below 5 to 10 mK. Above this region, the specific heat is dominated by the other mode (15) which in this region is roughly linear with a speed of transverse sound of 8.3×10^5 cm s^{-1} and gives a Debye T^3 behaviour.

4. Conclusions

We have calculated the transverse phonon spectrum for a three-dimensional Wigner crystal in a large magnetic field in the centred tetragonal structure. Our results indicate that if the ordered state is sufficiently crystalline there will be considerable

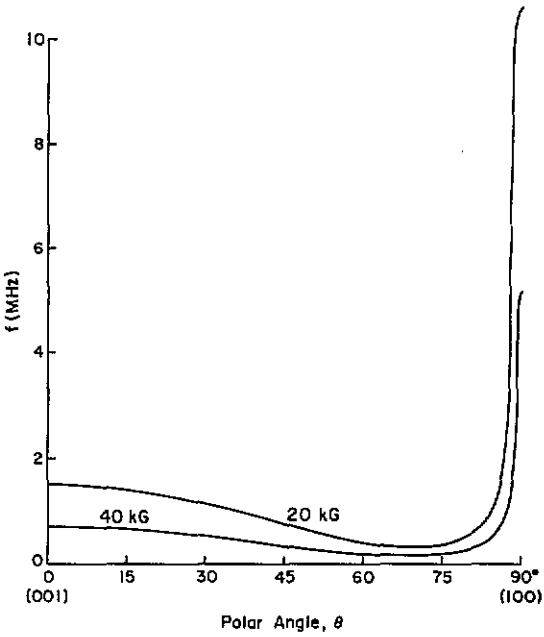

Figure 5. Variation of the frequency of one of the transverse modes with polar angle. The magnitude of q was fixed at $\pi/(5c)$. When q points along the (100) direction the mode is polarized along (010), while for q in the (001) direction the mode has polarization vector $\hat{\epsilon} = (1, i, 0)$.

amount of anisotropy in the transverse modes for q perpendicular to the magnetic field. This would be an indication that the ground state is indeed crystalline. Measurements of the critical field for depinning [21] seem to indicate a crystallite size of the order of tens of micrometres. By cooling through the transition in an electric field it may be possible to increase the size of the crystal domains, much as high quality ionic crystals are grown.

If the crystal is in a HCP or glassy structure, then this anisotropy will be absent and the phonon spectrum will not tell us much about the crystallinity of the ordered state. However, the detection of these transverse modes will indicate that the Coulomb forces are sufficiently strong even in the presence of disorder to produce the finite shear modulus that is characteristic of a solid.

Because of the extremely large magnetic field, which actually affects the strength of the shear response, the phonons are quite different from those of a conventional solid. The mode frequencies are very strong functions of the angle between the wavevector and the magnetic field. The frequencies vary as q^2 rather than linearly with q at long wavelengths, leading to a specific heat which varies as $T^{3/2}$ instead of the usual T^3 Debye law. In addition the specific heat will vary as $H^{3/2}$ at the lowest temperatures.

Acknowledgments

I would like to thank Tom Rosenbaum, Bellave Shivaram, Steve Kivelson and David DiVincenzo for useful discussions. This work was supported by the Louisiana Educational Quality Support Fund under grant LEQSF(1989-92)-RD-A-1.

References

[1] Wigner E P 1934 *Phys. Rev.* **46** 1002
[2] Clark C B 1968 *Phys. Rev.* **109** 1133
[3] Coldwell-Horsfall R A and Maradudin A A 1960 *J. Math. Phys.* **1** 395
[4] Carr W J 1961 *Phys. Rev.* **122** 1437
[5] de Wette F W 1964 *Phys. Rev.* A **135** 287
[6] Care C M and March N H *1975 Adv. Phys.* **24** *101*
[7] Bonsall L and Maradudin A A 1977 *Phys. Rev.* B **15** 1959
[8] Grimes C C and Adams G 1979 *Phys. Rev. Lett.* **42** 795
[9] Stan M A and Dahm A 1989 *Phys. Rev.* B **40** 8995
Hu X L and Dahm A 1990 Physica B **165** 839
[10] Durkan J, Elliot R J and March N H 1968 *Rev. Mod. Phys.* **40** 812
Ruderman M A 1968 *Nature* **223** 1128
[11] Tsui D C, Störmer H L and Gossard A C 1982 *Phys. Rev. Lett.* **48** 1559
[12] Lam P K and Girvin S M 1984 *Phys. Rev.* B **30** 473
Levesque D, Weis J J and MacDonald A H 1984 *Phys. Rev.* B **30** 1056
Chui S T, Hakim T M and Ma K B 1986 *Phys. Rev.* B **33** 7110
Esfarjani K and Chui S T 1990 *Phys. Rev.* B **42** 10758
[13] Andrei E Y, Deville G, Glattli D C, Williams F I B, Paris E and Etienne B 1988 *Phys. Rev. Lett.* **60** *2765*
Willet R L, Störmer H L, Tsui D C, Pfeiffer L N, West K W and Baldwin K W 1988 *Phys. Rev.* B **39** 7881
Goldman V J, Shayegan M and Tsui D C 1988 *Phys. Rev. Lett.* **61** 881
Jiang H W, Willet R L, Störmer H L, Tsui D C, Pfeiffer L N and West K W 1990 Phys. Rev. Lett. **65** 633
Goldman V J, Santos M, Shayegan M and Cunningham J E 1990 *Phys. Rev. Lett.* **65** 2189
Paalanen M A, Willet R L, Littlewood P B, Ruel R R, West K W, Pfieffer L N and Bishop D J 1992 in preparation
[14] Kaplan J I and Glasser M L 1972 *Phys. Rev. Lett.* **28** 1077
Kleppman W G and Elliot R J 1975 *J. Phys. C: Solid State Phys.* **8** 2729
[16] Doman B G S 1979 *J. Phys. C: Solid State Phys.* **12** 1521
[17] Kuramoto Y 1978 *J. Phys. Soc. Japan* **44** 1572
[18] MacDonald A H and Bryant G W 1987 *Phys. Rev. Lett.* **58** *515*
[19] Sommerford D J 1971 *J. Phys. C: Solid State Phys.* **4** 1570
[20] Ruderman M 1971 *Phys. Rev. Lett.* **27** 1306
[21] Rosenbaum T F, Field S B, Nelson D A and Littlewood P B 1985 *Phys. Rev. Lett.* **54** 241
Field S B, Reich D H, Shivaram B S and Rosenbaum T F 1986 *Phys. Rev.* B **33** 5082
[22] Schlicht B and Nimtz G 1982 *Physics of Narrow Gap Semiconductors (Lecture Notes in Physics 152)* ed E Gornik, H Heinrich and L Palmetshofer (Berlin: Springer) p 383
[23] Stadler J P and Nimtz G 1986 *Phys. Rev. Lett.* **56** 382
[24] Goldman V J, Drew H D, Shayegan M and Nelson D A 1986 *Phys. Rev. Lett.* **56** 968
[25] Aleinikov A P, Baranskii P I and Zhidkov A V 1982 *Pis. Zh. Eksp. Teor. Fiz.* **35** 464 (Engl. Transl. 1988 *JETP Lett.* **35** 574)
[26] Raymond A, Robert J L, Aulombard R L, Bousquet C and Valassiades O 1982 *Physics of Narrow Gap Semiconductors (Lecture Notes in Physics 152)* ed E Gornik, H Heinrich and L Palmetshofer (Berlin: Springer) p 387
[27] Elliot R J and Kleppman W G 1975 *J. Phys. C: Solid State Phys.* **8** 2735
[28] Care C M and March N H 1971 *J. Phys. C: Solid State Phys.* **4** L372
[29] Kuramoto Y 1979 *J. Phys. C: Solid State Phys.* **12** 2033
[30] Glyde H R and Keech G H *1980 Ann. Phys.* **127** *330*
[31] Schiff L H 1968 *Quantum Mechanics* (New York: McGraw-Hill) p 261
[32] Born M and Huang K 1959 *Dynamical Theory of Crystal Lattices* (Oxford: Oxford University Press) ch 3
[33] Côté R and MacDonald A H 1990 *Phys. Rev. Lett.* **65** 2662
Esfarjani K and Chui S T 1991 *J. Phys.: Condens. Matter* **3** 5825